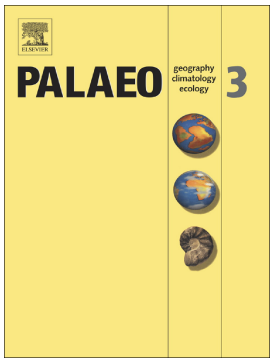

Population response during an Oceanic Anoxic Event: The case of Posidonotis (Bivalvia) from the lower Jurassic of the Neuquén Basin, Argentina

Sonia Ros Franch, Javier Echevarría, Susana E. Damborenea, Miguel O. Manceñido, Hugh C. Jenkyns, Aisha Al-Suwaidi, Stephen P. Hesselbo, Alberto C. Riccardi

PII: S0031-0182(19)30141-5
DOI: https://doi.org/10.1016/j.palaeo.2019.04.009
Reference: PALAEO 9153

To appear in: *Palaeogeography, Palaeoclimatology, Palaeoecology*

Received date: 11 February 2019
Revised date: 5 April 2019
Accepted date: 8 April 2019

Please cite this article as: S.R. Franch, J. Echevarría, S.E. Damborenea, et al., Population response during an Oceanic Anoxic Event: The case of Posidonotis (Bivalvia) from the lower Jurassic of the Neuquén Basin, Argentina, Palaeogeography, Palaeoclimatology, Palaeoecology, https://doi.org/10.1016/j.palaeo.2019.04.009

Population response during an Oceanic Anoxic Event: the case of *Posidonotis* (Bivalvia) from the Lower Jurassic of the Neuquén Basin, Argentina

Sonia Ros Franch[a*], Javier Echevarría[a], Susana E. Damborenea[a], Miguel O. Manceñido[a], Hugh C. Jenkyns[b], Aisha Al-Suwaidi[c], Stephen P. Hesselbo[d], Alberto C. Riccardi[a]

[a]División Paleozoología de Invertebrados, Museo de La Plata, Consejo Nacional de Investigaciones Científicas y Técnicas (CONICET), Paseo del Bosque s/n, A1900FWA La Plata, Argentina.

[b]Department of Earth Sciences, University of Oxford, South Parks Road, Oxford OX1 3AN, United Kingdom.

[c] Department of Earth Sciences, Khalifa University of Science and Technology, PO Box 127788, Abu Dhabi, United Arab Emirates.

[d]Camborne School of Mines and Environment and Sustainability Institute, University of Exeter, Penryn Campus, Penryn, Cornwall TR10 9FE, United Kingdom.

*Sonia Ros Franch (corresponding author) e-mail: soniaros@fcnym.unlp.edu.ar

Javier Echevarría e mail: javierechevarria@fcnym.unlp.edu.ar

Susana E. Damborenea e-mail: sdambore@fcnym.unlp.edu.ar

Miguel O. Manceñido e-mail: mmanceni@fcnym.unlp.edu.ar

Hugh C. Jenkyns e-mail: hughj@earth.ox.ac.uk

Aisha Al-Suwaidi e-mail: aisha.alsuwaidi@ku.ac.ae

Stephen P. Hesselbo e-mail: S.P.Hesselbo@exeter.ac.uk

Alberto C. Riccardi e-mail: riccardi@fcnym.unlp.edu.ar

Abstract. Benthonic marine species show a wide range of biological reactions to seawater chemical changes through time, from subtle adjustments to extinction. The Early Toarcian Oceanic Anoxic Event (T-OAE) was recently recognized in the Neuquén Basin, Argentina, confirming its global scope. The event was identified

chemostratigraphically on the basis of a relative increase in marine organic carbon and a characteristic negative carbon-isotope excursion ($\delta^{13}C_{org}$) in bulk rock and fossil wood in the upper Pliensbachian–lower Toarcian interval in the Arroyo Lapa section (Neuquén). Simultaneously with collection of lithological samples, a high-resolution biostratigraphical survey was carried out, and the scarce benthonic fauna was collected in order to check the biotic response to changing marine geochemical conditions. We present here an analysis of size and abundance data from the T-OAE interval in the Neuquén Basin for the dominant bivalve species, the paper-clam *Posidonotis cancellata* (Leanza), and relate these data to geochemical proxies (%TOC and $\delta^{13}C_{org}$) obtained at the same locality. The abundance of *P. cancellata* increased when the rest of the benthos diminished, reaching a maximum at the onset level of the T-OAE, and then decreasing. Size-frequency distributions show a noteworthy lack of juvenile shells. Shell size shows a positive correlation with %TOC in the whole section, though over the T-OAE interval proper, it decreases below the level where the maximum %TOC value is attained and increases above it. *Posidonotis cancellata* shows features of opportunistic species, such as high tolerance to hypoxia, strong dominance in impoverished environments and a strong dependence on primary productivity, but at the same time had a reproductive strategy more similar to equilibrium species, with relatively low juvenile mortality rates. Several anatomical features suggest adaptation to permanently dysaerobic environments. The species disappeared just before the minimum negative carbon-isotope value was reached; and by the same time the genus became extinct worldwide.

Key words: Toarcian OAE, opportunistic species, biotic reactions, paper-clams, South America.

1. Introduction

A relatively high extinction rate affecting various sorts of organisms was recorded around the world for the late Pliensbachian–early Toarcian interval, with a peak at the Tenuicostatum/Falciferum ammonite zonal boundary (Raup and Sepkoski, 1984; Hallam, 1986; Sepkoski and Raup, 1986; Little and Benton, 1995; Hallam and Wignall, 1997; Harries and Little, 1999; Aberhan and Fürsich, 2000; Macchioni and Cecca, 2002; Cecca and Macchioni, 2004; Boomer et al., 2008; Caswell et al., 2009; Dera et al., 2010; Guex et al., 2012; Fantasia et al., 2018). This early Toarcian extinction event has been linked to the Early Toarcian Oceanic Anoxic Event (T-OAE) (Hallam, 1986, 1987; Aberhan and Baumiller, 2003; Wignall et al., 2005; Gómez et al., 2008; Bond and Wignall, 2014) and/or to global warming (Bailey et al., 2003; Dera et al., 2009; Dera and Donadieu, 2012; García Joral et al., 2011; Gómez and Goy, 2011; Danise et al., 2013; Krencker et al., 2015; Dunhill et al., 2018). The T-OAE was characterized by widespread deposition of shales rich in organic carbon, a negative carbon-isotope excursion (CIE) typically intersecting an overall positive shift, local euxinic conditions and seawater temperature rise (Jenkyns, 1985, 1988, 2003, 2010; Jenkyns and Clayton, 1986, 1997; Hesselbo et al., 2000, 2007; Hermoso et al., 2009; Danise et al., 2013; Xu et al., 2018), and is regarded as one of the most significant environmental perturbations of the Mesozoic Era.

The ecological consequences of this particular extinction event are relevant to understanding how all the inter-connected environmental changes may have affected marine organisms (Röhl et al., 2001; Caswell et al., 2009; Morten and Twitchett, 2009; Dera et al., 2010; Fraguas and Young, 2011; García Joral et al., 2011; Danise et al., 2013; Caswell and Frid, 2013, 2016; Caswell and Coe, 2014; Danise et al., 2019).

Abundance and body size are two ecologically related parameters that have been studied in this context. It has been suggested that body size was related to extinction dynamics in different organisms (McKinney, 1990, 1997; Jablonski, 1996; Payne, 2005; Twitchett, 2007; Harries and Knorr, 2009; Piazza et al., 2019). In this context, there are a few analyses of the effects on size and other morphological features of marine invertebrates and vertebrates during the early Toarcian extinction event (Morten and Twitchett, 2009; Maxwell and Vincent, 2015; García Joral et al., 2018). For example, detailed quantitative studies on abundance and size on populations of the bivalves *Bositra radiata* (Goldfuss) and *Pseudomytiloides dubius* (Sowerby) from T-OAE black shales in Yorkshire, UK, in relation to geochemical proxies, yielded insightful results (Caswell and Coe, 2013) that can be compared with those presented here.

The genus *Posidonotis* Losacco, 1942 (including its junior synonym *Pectinula* Leanza, 1943) has a stratigraphic range restricted to the Lower Jurassic (upper Sinemurian to lower Toarcian). Its distribution was reviewed by Damborenea (1989) and Aberhan and Pálfy (1996): in North America, for example, the genus occurs in upper Sinemurian to lower Toarcian beds, whilst in South America and elsewhere it is restricted to upper Pliensbachian to lower Toarcian deposits (Fig. 1). Although most abundant in temperate regions of the eastern Palaeo-Pacific, it has also sporadic occurrences in central Tethys (Italy: Losacco, 1942; Monari, 1994; Greece: Damborenea, 1987), and Japan (Hayami, 1988; Tanabe, 1991), but it appears to be absent from very high palaeolatitudes. The Tethyan and Japanese records were attributed by Aberhan and Pálfy (1996) to eastward migration along the Hispanic Corridor and subsequent isolation. Although this was the most probable migration route for benthonic bivalves (Damborenea and Manceñido, 1979), *Posidonotis* distribution data may also be explained by dispersion across the Pacific following the westward

direction of prevailing currents (Damborenea et al., 2013, fig, 6.4). Throughout its geographical and temporal range, *Posidonotis* commonly occurs forming monospecific shell pavements in dark/black shales. The functional morphology, facies distribution and palaeoecology of *Posidonotis* species were extensively discussed by Damborenea (1987, 1989) and Aberhan and Pálfy (1996), who regarded them as opportunistic species characteristic of quiet-water, dysaerobic environments.

The species *Posidonotis cancellata* (Leanza) was systematically revised by Damborenea (1987) and was then provisionally regarded as a distinct species on the basis of subtle morphological differences. On the other hand, Aberhan and Pálfy (1996) considered it as a subjective synonym of the long-ranging *P. semiplicata* (Hyatt). In Argentina, the species has a very wide geographical distribution from San Juan Province in the north to Chubut Province in the south (location of records from Mendoza and Neuquén provinces are shown in Fig. 1B), although it is restricted stratigraphically to the uppermost Pliensbachian–lowermost Toarcian interval (*Fanninoceras disciforme* to Tenuicostatum Zones). The type-species of the genus, *Posidonotis dainelli* Lossaco was present in the Mediterranean (Greece and Italy) Tethys (Losacco, 1942; Damborenea, 1987, 1989; Monari, 1994) and Japan (Hayami, 1988; Tanabe, 1991) in comparable sedimentary environments at about the same time (Izumi et al., 2012).

Recently, the sedimentary record of the T-OAE was recognized in the Neuquén Basin, Argentina (Fig. 1), confirming the event as a global phenomenon (Al-Suwaidi et al., 2010, 2016). The event was identified chemostratigraphically on the basis of a relative increase in marine organic carbon and a characteristic overall positive excursion, intersected by a negative carbon-isotope excursion ($\delta^{13}C_{org}$) in bulk rock and fossil wood. High-resolution sampling with tight biostratigraphical control (ammonites,

Riccardi, 2008a, 2008b) was carried out in the upper Pliensbachian/lower Toarcian interval in the Arroyo Lapa section (Fig. 2), where benthonic species are scarce.

Although other authors have suggested a general correlation between degree of oxygenation and shell size for *Posidonotis* species (e.g., Aberhan and Pálfy, 1996) no statistical analysis had been attempted prior to this study. Hence, we here present a thorough analysis of size and abundance data from the T-OAE interval in the Neuquén Basin for the dominant bivalve species, the paper-clam *Posidonotis cancellata* (Leanza), and relate these data to geochemical proxies [total organic carbon (%TOC) and $\delta^{13}C_{org}$].

2. Geological setting

The Neuquén Basin is an extensive Mesozoic back-arc basin developed on the western convergent margin of the South American plate (Legarreta and Uliana, 1996; see also Fig. 1), in connection with the break-up of Gondwana (Uliana and Biddle, 1988). After initial rifting (spanning the Late Triassic to earliest Jurassic), during the sag phase (Sinemurian to Toarcian) the coalescence of formerly unconnected half-grabens took place with widespread transgression over most of the Neuquén embayment (Vergani et al., 1995; Legarreta and Uliana, 1996).

The presence of a well-developed Lower Jurassic succession at Arroyo Lapa (Charahuilla-Chacaico area) was recognized long ago (e.g., Weaver, 1931, p. 27-29; Groeber et al., 1953, p. 158-161; Volkheimer, 1973). There, the Lower–Middle Jurassic Cuyo Group attains about 1500 m in thickness. From the lithostratigraphical point of view, the interval considered in this study is consistently assigned to the Los Molles Formation (Weaver, 1931; see also Riccardi and Damborenea, 1993; Gulisano and Gutiérrez-Pleimling, 1995; Arregui et al., 2011). Furthermore, paleomagnetic data obtained from this section were used to build a composite magnetostratigraphy for the

Early Jurassic of the Neuquén Basin (Iglesia Llanos and Riccardi, 2000). Riccardi (2005) and Manceñido et al. (2007) first reported the occurrence of organic-rich dark shales probably representing the T-OAE in this section, which was subsequently confirmed with detailed sedimentological and geochemical evidence by Al-Suwaidi et al. (2010, 2016, see above).

The surveyed section of the Los Molles Formation (Fig. 2A) starts with conglomerates overlying tuffs of the Lapa Formation, followed by about 80 m of lower Pliensbachian deposits dominated by sandstones with interbedded siltstones. Upper Pliensbachian deposits comprise about 150 m of heterogeneous siliciclastic and pyroclastic sediments of alternating sandstones, siltstones and tuffs. The next package, over 70 m thick, spans the latest Pliensbachian to earliest Toarcian time interval, and consists of laminated black shales and siltstones interbedded with relatively thin sandstone layers (Fig. 2B, further description in Al-Suwaidi et al., 2010). This last interval was logged and sampled in detail and provided the data for this study.

3. Material and methods

3.1.Material

The analysis performed here was restricted to material from the Arroyo Lapa South section, because detailed geochemical data (published by Al-Suwaidi et al., 2010) were obtained from rock samples taken simultaneously as the paleontological samples (Ros-Franch et al., 2014). Albeit additional detailed data for the T-OAE interval are available (Al-Suwaidi et al., 2016), they were not used here in order to maintain statistical consistency, since they only cover a minor (upper) part of the stratigraphic range of *P. cancellata* in the logged section. The fossil material is deposited in the Invertebrate Palaeontology collection of the La Plata Museum (MLP 35869 to 35903).

Size data were obtained from 502 photographed individual valves. Shell length and surface area (Fig. 3) were measured using ImageJ software (http://rsb.info.nih.gov/ij/). A synthesis of the data used is shown in Table 1. Abundance data were recorded as: (a) area covered by specimens on each slab/slab surface area (Fig. 4); (b) number of specimens present per dm^2 of each slab surface.

3.2. Variables analyzed

The main goal of the present paper is to check for responses in *Posidonotis* populations associated to variations in total organic carbon (%TOC) and carbon-isotope ($\delta^{13}C_{org}$) ratios. %TOC can potentially indicate changes in primary production, assuming that this quantity factor is the first-order control on organic-matter flux to the sea floor and subsequent burial, rather than variable preservation (cf. Demaison and Moore, 1980; Pedersen and Calvert, 1990). Variations in bulk $\delta^{13}C$, if recording global changes in the ocean–atmosphere system, should relate to ρCO_2, which will be drawn down during episodes of global organic-matter burial such as the T-OAE, if not counterbalanced by methanogenic and/or volcanic sources, to which the characteristic negative excursion is usually ascribed (Hesselbo et al., 2000; McElwain et al., 2005; Hermoso et al., 2012; Trecalli et al., 2012; Ullmann et al., 2014). Evidence for volcanism, which would have supplied CO_2 to the atmosphere, is given by the stratigraphic association of relatively elevated contents of mercury within sediments deposited during the T-OAE in many places, including Arroyo Lapa South, with an ultimate source suggested as the Karoo–Ferrar Large Igneous Province (Percival et al., 2015, 2016).

When checking for association between population and environmental variables, two options were considered: direct correlation to the variable (comparison with %TOC

and $\delta^{13}C_{org}$ closest to the *Posidonotis* sample) and correlation to trends on the variables (first %TOC and $\delta^{13}C_{org}$ value after the *Posidonotis* sample minus immediate previous values, Table 1, columns "dif. %TOC" and "dif. $\delta^{13}C_{org}$"; when the *Posidonotis* sample coincided with a geochemical sample, the trend was determined as sample value minus the immediate previous value).

Variables analyzed for *Posidonotis* samples (Table 1) were individual sizes distribution and population density. Only samples with at least five measured shells were considered. Maximum size was quantified as maximum-length per sample, and five maximum-length values per sample. Maximum-length per sample is often used as a size estimator (e.g., Hallam, 1975; Aberhan and Fürsich, 1997; Morten and Twitchett, 2009), but it can be strongly influenced by outliers. Hence, the analyses were also performed on the five largest measurements per sample. Nevertheless, these two data sets seem to be dependent on sample size (for maximum length Spearman's $r_s = 0.53$, $p = 0.022$; for 5 maximum lengths $r_s = 0.52$, $p<0.01$); *i.e.*, the larger the sample, the higher the probability of finding large shells.

For length-data distribution, the medians, variances, skewness and kurtosis were also considered. Anderson (2001) used size variance as an estimate of size range, but also as a proxy for maximum size. Since the lowest value is bounded (values less than zero being impossible), variance will increase primarily due to larger values. Variance will also be less sensitive to outliers than maximum length. Levene's test for homogeneity of variances shows significant differences either based on means or medians ($p<0.01$), and there seems to be no correlation between sample size and variance ($r_s = 0.38$, $p = 0.12$).

3.3. Methodology

The geochemical variables and the size and abundance data are expected to be responding to the same environmental factors (those responsible for the OAE); hence a monotonic (not necessarily linear) association should be expected among these sets of variables. The non-parametric Spearman rank-order correlation coefficient (r_s) was used to check that association. A correlation analysis was also performed for size and abundance data with reference to stratigraphic position during the T-OAE portion of the section, to check for trends over time.

From the differences within the geochemical variables (Table 1, columns "dif. %TOC" and "dif. $\delta^{13}C_{org}$"), another analysis was proposed in order to compare with the results provided by Caswell and Coe (2013) for *Bositra radiata*. The samples were grouped in positive and negative differences for both geochemical variables (treated as increasing and decreasing trends), and the length-frequency distributions for both groups were compared by means of a Kolmogorov–Smirnov test (to check for equality of distribution) and Mann–Whitney U test (to check for equality of medians). All analytical methods are described in Hammer and Harper (2006) and were performed on PAST 3.20 (Hammer et al., 2001).

4. Results

The typical matrix of *Posidonotis cancellata* consists of fairly thin-layered, dark shales, bearing monospecific pavements, made up of flat-lying, concordant valves (Fig. 2C). The valves are fragile, thin-shelled, usually unbroken (even if disarticulated), which suggests undisturbed, autochthonous accumulation. Most commonly, specimens appear as internal and external moulds (Fig. 4B), although in some instances delicate shell remains are preserved as white paper-thin laminae (Fig. 4C).

Size and abundance data show a general correspondence (Fig. 5), though only the 5 maximum-length values show a significant negative response to values of, and changes in, $\delta^{13}C_{org}$ (Table 2). These results seem to be dependent on sample size. Skewness, on the other hand, seems to be positively correlated with %TOC values.

Comparison of groups of samples under increasing and decreasing trend contexts in geochemical variables (Fig. 6) shows a significant difference in distribution and median for both %TOC (Kolmogorov–Smirnov test $p<0.01$; Mann-Whitney U test $p<0.01$) and $\delta^{13}C_{org}$ (Kolmogorov–Smirnov test $p<0.01$; Mann-Whitney U test $p<0.01$), with a larger median during positive shifts of %TOC and during negative excursions in $\delta^{13}C_{org}$.

Abundance measured as number of specimens on an area of 1 dm^2 shows a weak positive correlation with %TOC, which seems close to, though not reaching, significance (Table 2).

Correlation between size and stratigraphic position during the T-OAE shows a two-stage pattern (displayed on Fig. 5): an initial one (between about 54 and 58 m from the base, before the maximum %TOC positive peak) of decreasing size (all samples: $r_s = -0.23$, $p < 0.001$; maximum sizes only: $r_s = -0.96$, $p = 0.003$) and a final one (between about 61 and 62 m from the base, after the %TOC positive peak) of increasing size (all samples: $r_s = 0.5117$, $p = 0.001$; maximum sizes only: $r_s = 1$, $p = 0.33$). Abundance shows an overall decreasing trend ($r_s = -0.76$, $p = 0.01$) within the T-OAE interval.

5. Discussion

5.1. Opportunistic behaviour in Posidonotis cancellata

Several authors have suggested opportunistic behaviour for *Posidonotis* inferred from its mode of occurrence (Hallam, 1977, p. 62, as *Pectinula*; Damborenea, 1987, p.

196; Aberhan, 1993, p. 119; Aberhan and Pálfy, 1996, p. 999). Opportunistic taxa show some particular features, such as high fecundity and short generation time, high intrinsic rates of population increase and a generalistic physiology, which allow them to rapidly increase in number in response to environmental perturbations (Levinton, 1970). Their recognition in the fossil record is not always easy, but *P. cancellata* clearly shows some of the main features of opportunistic species. It tends to appear in the logged sections as the dominant and usually the only species in thin but widespread isochronous horizons, a feature typical of opportunistic taxa (Levinton, 1970). The presence of 1–2 species of epifaunal suspension feeders at a particular horizon is comparable with the "peak of opportunist" in present-day deoxygenated areas (Caswell and Frid, 2016). During ecological crises, opportunistic species tend to appear in these monotypic associations in higher frequency (Kauffman and Erwin, 1995; Kauffman and Harries 1996, fig. 1). Although *P. cancellata* appears in the studied section at least 30 metres below the onset of the T-OAE, it is noteworthy that the higher frequencies of levels and higher abundance of specimens per level are attained during the interval recording the event itself (Fig. 5).

Fecundity and generation time are hard, if not impossible, to observe in the fossil record of most organisms. Nevertheless, fossil-association data, like the size-frequency distributions, may provide some insights on the matter (Levinton and Bambach, 1970). Taphonomic information points to autochthonous associations; no evidence of sudden burial was found on these beds, so that shell size can be related to relative time of death (Levinton and Bambach, 1970). Even though some time averaging may have occurred, *P. cancellata* beds are thin, implying short time intervals and little variations in population dynamics; unimodal samples may even represent single cohorts.

The scarcity of small shells is remarkable in the size-frequency distributions of *P. cancellata*. The smallest shell measured is about 3mm long, indicating probably the smallest measurable size; but when the distribution of the samples is analyzed (Fig. 6) it is clear that the smallest sizes, larger than that threshold, are less abundant. Taphonomic biases can be disregarded, either selective transport (both sedimentological and taphonomic evidence point to a rather quiet-water environment) or selective dissolution (dissolution affected many of the samples, but external moulds were nonetheless preserved). Present-day opportunistic bivalve species usually have the highest frequency in their smallest categories, a reflection of a high juvenile mortality rate (Levinton and Bambach, 1970). Various species studied for the same time interval in other parts of the world also show most individuals concentrated in the smaller size-classes, such as *Bositra radiata* and *Pseudomytiloides dubius* from northern England (Caswell and Coe, 2013), or *Bositra buchi* (Römer) from southwest Germany (Röhl et al., 2001). *Posidonotis cancellata* size-frequency distributions suggest that juvenile mass mortality was not particularly high in any of the populations, and mortality rates were relatively constant through time, a feature more typical of equilibrium species. Size-frequency distributions for increasing *vs* decreasing %TOC settings differ due to the differences in size; when the mean is subtracted from each sample, the Kolmogorov–Smirnov test shows no significant differences in distribution ($p = 0.82$). From this result, it can be concluded that only size was affected by the environmental variables analyzed here, while the reproductive strategy remained the same.

The larger median size under an increasing %TOC context (Fig. 6), together with the positive correlation of skewness with %TOC (Table 2, implying longer "positive" or right tails for length distribution in samples from environments with higher %TOC) can be related to more than one environmental variable. Percentage TOC

is one of the key characteristics used to recognize the impact of an Oceanic Anoxic Event (OAE) in the sedimentary record. The major driving force behind an OAE is supposed to have been an abrupt rise in global temperatures, probably forced by input of volcanogenic carbon dioxide, that in turn increased weathering of bedrock in subaerial and submarine environments and increased the flux of nutrients to the oceans: this would have caused an increase in organic productivity, favoring an intense oxygen demand in the water column and resulting in generalized hypoxia and increased rates of carbon burial (Jenkyns, 2010). The T-OAE, therefore, represents an interval of globally increased organic productivity during which oxygen-depleted waters characterized many marine environments, including those in the Neuquén Basin (Al-Suwaidi et al., 2010, 2016). The size increase in *Posidonotis* under increasing %TOC trends, as well as the highest abundance at the beginning of the T-OAE (Figs. 5 and 6), suggests an exploitation of plentifully available resources but, at the same time, a high tolerance to low-oxygen conditions. Although *P. cancellata* was occasionally present before oxygen levels began to decrease, its abundance increased as the rest of the benthos diminished.

Most current oxygen minimum zones (OMZ), where oxygen levels are permanently under 0.5 ml/L, show no monotonic shifts in body size for macrofauna along oxygen gradients, though in some polychaetes an increasing body size with decreasing oxygen trend has been found, which may be related to food availability (Levin, 2003). Caswell and Coe (2013) found a positive and significant regression slope of size on %TOC, similar to the results shown here, for *Pseudomytiloides dubius*. They also found an increase in size in *Bositra radiata* correlating with decreases in $\delta^{13}C_{org}$. Based on these and other responses to geochemical indicators, Caswell and Coe (2013) concluded that periods of higher primary productivity and greater oxygenation supported larger bivalves.

Hence, *Posidonotis cancellata* shows features of opportunistic species, like the high tolerance to hypoxia, its strong dominance in impoverished environments (preserved in thin extensive isochronous horizons), the strong dependence on primary productivity, but with a reproductive strategy more similar to equilibrium species (at least as regards the relatively low juvenile mortality rates).

5.2. Ecological response to the T-OAE

Macroinvertebrate faunal assemblages in the logged section are more diverse in the lower beds well below the level of the negative carbon-isotope excursion, showing a clear reduction on diversity upwards in the section. *Posidonotis cancellata* dominates (Fig. 5) the part of the section between its first record and the first T-OAE level (as identified by Al-Suwaidi et al., 2010, 2016). Apart from ammonites, only very rare *Entolium* sp., rhynchonellide and discinoid brachiopods are present in that stratigraphic interval. The latter are closely comparable to the species *Discinisca papyracea* (Goldfuss), known to occur in the lower Toarcian organic-rich shales from Swabia (Röhl et al., 2001; Schmidt-Röhl et al., 2002). At Arroyo Lapa, *Posidonotis* pavements become more abundant at the base of the T-OAE interval, intercalated with beds that in some places contain the free-living bivalve *Kolymonectes* sp. Although this last taxon may appear in dysaerobic facies in the Lower Jurassic deposits (Damborenea, 1998), it is recorded in the logged section only stratigraphically above the level of the main peak of %TOC and never forms shell-pavements. The stratigraphically highest *Posidonotis* is recorded at 63 m and the highest *Kolymonectes* at 64 m. The upward-following beds (between 64 and 69 m) show certain diversification of the fauna, containing very scarce inoceramids, lucinoids and pectinoids (*Entolium* sp.) as well as a few terebratulide brachiopods.

The abundance of *P. cancellata* reaches its highest values at the onset level of the T-OAE (Fig. 5), but it significantly decreases over the event interval up to where the taxon disappears. This stratigraphic distribution is congruent with observations on extant benthos, where densities of macrofauna are commonly depressed within the part of the OMZ where oxygen concentrations are lowest (Levin, 2003). Shell size, on the other hand, shows a two-stage response; though not strictly correlated with %TOC values in this portion of the log, it clearly shows a decreasing stratigraphic trend below the level of maximum %TOC and an increasing trend in higher levels; where %TOC reaches a maximum the species is not found. Despite surviving the conditions associated with highest %TOC, *P. cancellata* (and the whole genus) disappeared shortly thereafter, as shown by its highest occurrence in the section, in basal levels of the *Dactylioceras hoelderi* Zone (~ Serpentinum Standard Ammonite Zone).

Although the Lilliput effect (temporary body-size reduction linked to recovery events post-extinction; Twitchett, 2007; Harries and Knorr, 2009) is strictly applied for recovery events, several cases of size reduction are documented in connection with the Toarcian extinction event and also with other extinction events (e.g., Late Triassic extinction, Atkinson et al., 2019). Morten and Twitchett (2009) found a similar trend in *Pseudomytiloides dubius* from lower Toarcian sediments in northern England. That particular species apparently reached its smallest size during the late Serpentinum Zone, and disappeared shortly thereafter in the early Bifrons Zone. Fürsich et al. (2001) noticed the small size of *Parvamussium pumilum* (Lamarck) from the Toarcian of the Causses, and the same phenomenon was observed for *Bositra* and *Meleagrinella* in the T-OAE sediments of Canada (Martindale and Aberhan, 2017), and for *Bositra buchi* about the Elegans/Falciferum subzone boundary in Germany (Röhl et al., 2001). However, in other groups of organisms such as brachiopods, both decreasing and

increasing size trends were recorded prior to the early Toarcian extinction event (García Joral et al., 2018; Piazza et al., 2019) .

The overall stratigraphic size-trend observed in *P. cancellata* does not precisely correlate with any of the geochemical proxies, suggesting that environmental impoverishment should not be focused on these parameters alone, and wider oceanographic changes should be considered. Other global perturbations have been also suggested as causes of the early Toarcian extinction event. Heavily calcified organisms (*e.g.*, hermatypic corals, lithiotid bivalves, hypercalcified sponges) were selectively affected pointing to ocean acidification as another potential killing mechanism (cf. Trecalli et al., 2012; Hönisch et al., 2012).

Posidonotis disappeared in the section just before the minimum negative carbon-isotope values were attained (in the core of the OAE) and the genus never appeared again in the Neuquén basin. Taking into account its entire global stratigraphical range (Damborenea, 1987, 1989; Aberhan and Pálfy, 1996), the genus likely survived previous minor oceanic anoxic events, such as the Sinemurian–Pliensbachian and the Pliensbachian–Toarcian boundary events (Littler et al., 2010; Hesselbo et al., 2014; Percival et al., 2015) suggesting a relatively resilient taxon. Though *P. cancellata* survived the maximum % TOC peak of the T-OAE and even showed an increasing size trend thereafter, the abundance apparently followed a broadly decreasing pattern within the T-OAE itself.

Oxygen-poor conditions have been considered responsible for the smaller body sizes recorded in many bivalves during the Toarcian, probably due to increased juvenile mortality (Atkinson et al., 2019). Nevertheless, *P. cancellata* shows relatively low juvenile mortality and, furthermore, an increase of size that parallels %TOC. According to Levin (2003), metazoans in OMZ show some particular adaptations that allow them

to live in those environments, such as reduced blood-to-water diffusion distances, increased blood pigment affinity for oxygen, increased respiratory surfaces, and different strategies to avoid sinking in the soupy sediments typical of such environmental settings. *Posidonotis cancellata* shell morphology (and that of paper-clams in general) may be related to many of these adaptive needs; flat morphology entails a high surface/volume ratio, providing resistance to sinking, wide respiratory surfaces (mantle lobes apart from the ctenidia) with short diffusion distances. A teleplanic larval development, suggested for paper-clams, probably enabled these forms to migrate across oceanic barriers and also survive in black-shale environments (Oschmann, 1993). Metabolic adaptations cannot be identified in the fossil record, but the presence of haemoglobin in several species of bivalves belonging to different superfamilies might be invoked (Levin, 2003). If we also consider the unusual reproductive strategy (compared to other opportunistic species), it is possible that *P. cancellata* (and also the entire genus *Posidonotis*) actually represents a taxon adapted to permanent hypoxia, similar to the fauna of modern OMZs, and not to periodic hypoxia, more typical of opportunistic species. This behaviour could also explain the widest geographical distribution of the genus during the late Pliensbachian to early Toarcian time interval (Fig. 1). If that were the case, the extinction of the taxon might have been related to the environmental change driven by the end (rather than by the onset) of the T-OAE. It should be considered that the T-OAE was linked to a mass extinction event and many studies show a systematic reorganization of communities thereafter (Aberhan and Fürsich, 1997; Danise et al., 2013; Caswell and Frid, 2016; Danise et al., 2019); it is possible, therefore, that after this crisis this particular taxon could not adapt to the conditions of the new ecosystems. On the other hand, it is also possible that within the

T-OAE the oxygen level may have dropped beyond the minimum of ecological tolerance for *Posidonotis cancellata*.

6. Conclusions

The study of the size and abundance distribution of *Posidonotis cancellata* in relation with the environmental parameters determined from a section in the Neuquén Basin of Argentina shows a significantly larger shell under conditions of increasing content of total organic carbon. Abundance reaches a maximum at the beginning of the T-OAE, and then decreases till the disappearance of the species in the section. Size-frequency distribution and taphonomic information indicate that juvenile mass mortality was not particularly high in any population and mortality rates were relatively constant through time. Shell size decreases up to the level of maximum %TOC and, higher in the section, a size increase was observed to just below the extinction level of the species.

Posidonotis cancellata shows features of opportunistic species, like the high tolerance to hypoxia, the strong dominance in impoverished environments and the strong dependence on primary productivity but, on the other hand, also shows a reproductive strategy more similar to equilibrium species, with relatively low juvenile mortality rates. *Posidonotis cancellata* shows several adaptations to low-oxygen environments, like a flat morphology (providing a high surface/volume ratio, resistance to sinking, wide respiratory surfaces and short diffusion distances). The taxon may then represent a species adapted to permanent hypoxia, similar to modern faunas in oxygen minimum zones. Such ecology could explain the widespread distribution of these bivalves during latest Pliensbachian–earliest Toarcian time (interval/s of widespread hypoxia) and its extinction when environmental conditions changed. This kind of

analysis may help to improve understanding of biotic responses to large environmental disturbances under conditions of global warming, such as exist today.

Acknowledgements

This research was funded by Consejo Nacional de Investigaciones Científicas y Técnicas (CONICET). Hesselbo and Jenkyns acknowledge funds from the Royal Society of London for a joint International Project with La Plata University. We also thank two anonymous reviewers and editor Thomas Algeo who provided helpful suggestions to improve the text. This work is a contribution to the Project IGCP-655 of the UNESCO-IUGS.

References

Aberhan, M., 1993. Benthic macroinvertebrate associations on a carbonate-clastic ramp in segments of the Early Jurassic back-arc basin of northern Chile (26-29ºS). Rev. Geol. Chile 20, 105–136.

Aberhan, M., Baumiller, T.K., 2003. Selective extinction among Early Jurassic bivalves: a consequence of anoxia. Geology 31, 1077–1080.

Aberhan, M., Fürsich, F.T., 1997. Diversity analysis of Lower Jurassic bivalves of the Andean Basin and the Pliensbachian-Toarcian mass extinction. Lethaia 29, 181–195.

Aberhan, M., Fürsich, F.T., 2000. Mass origination versus mass extinction: the biological contribution to the Pliensbachian-Toarcian extinction event. J. Geol. Soc., London 157, 55–60.

Aberhan, M., Pálfy, J., 1996. A low oxygen tolerant East Pacific flat clam (*Posidonotis semiplicata*) from the Lower Jurassic of the Canadian Cordillera. Can. J. Earth Sci. 33, 993–1006.

Al-Suwaidi, A.H., Angelozzi, G.N., Baudin, F., Damborenea, S.E., Hesselbo, S.P., Jenkyns, H.C., Manceñido, M.O., Riccardi, A.C., 2010. First record of the Early Toarcian Oceanic Anoxic Event from the Southern Hemisphere, Neuquén Basin, Argentina. J. Geol. Soc., London 167, 633–636.

Al-Suwaidi, A.H., Hesselbo, S.P., Damborenea, S.E., Manceñido, M.O., Jenkyns, H.C., Riccardi, A.C., Angelozzi, G.N., Baudin, F., 2016. The Toarcian Oceanic Anoxic Event (Early Jurassic) in the Neuquén Basin, Argentina: A Reassessment of Age and Carbon Isotope Stratigraphy. J.Geol. 124, 171–193.

Anderson, L.C., 2001. Temporal and geographic size trends in Neogene Corbulidae (Bivalvia) of tropical America: using environmental sensitivity to decipher causes of morphologic trends. Palaeogeogr. Palaeoclimatol. Palaeoecol. 166, 101–120.

Arregui, C., Carbone, O., Martínez, R., 2011. El Grupo Cuyo (Jurásico Temprano-Medio) en la Cuenca Neuquina. Geología y Recursos Naturales de la Provincia del Neuquén. Relatorio del 18° Congreso Geológico Argentino. Buenos Aires, p. 77–89.

Atkinson, J.W., Wignall, P.B., Morton, J.D., Aze, T., 2019. Body size changes in bivalves of the family Limidae in the aftermath of the end-Triassic mass extinction: the brobdingnag effect. Palaeontology 1–22. doi: 10.1111/pala.12415

Bailey, T.R., Rosenthal, Y., McArthur, J.M., van de Schootbrugge, B., Thirlwall, M.F., 2003. Paleoceanographic changes of the Late Pliensbachian-Early Toarcian

interval: a possible link to the genesis of an Oceanic Anoxic Event. Earth Planet. Sci. Lett. 212, 307–320.

Bond, D.P.G., Wignall, P.B., 2014. Large igneous provinces and mass extinctions: an update. Pp. 29–56. In: Keller, G., Kerr, A.C. (Eds.), Volcanism, Impacts and Mass Extinctions: Causes and Effects. Geol. Soc. Am., Spec. Pap. 505, 29–55.

Boomer, I., Lord, A., Crasquin, S., 2008. The extinction of the Metacopina (Ostracoda). Senckenbergiana Lethaea 88, 47–53.

Cao, W., Zahirovic, S., Flament, N., Williams, S., Golonka, J., Müller, R. D., 2017. Improving global paleogeography since the late Paleozoic using paleobiology. Biogeosciences 14, 5425–5439.

Caswell, B.A., Coe, A.L., 2013. Primary productivity controls on opportunistic bivalves during Early Jurassic oceanic deoxygenation. Geology 41, 1163–1166.

Caswell, B.A., Coe, A.L., 2014. The impact of anoxia on pelagic macrofauna during the Toarcian Oceanic Anoxic Event (Early Jurassic). Proc. Geol. Assoc. 125, 383–391.

Caswell, B.A., Frid, C.L.J., 2013. Learning from the past: functional ecology of marine benthos during eight million years of aperiodic hypoxia, lessons from the Late Jurassic. Oikos 122, 1687–1699.

Caswell, B.A., Frid, C.L.J., 2016. Marine ecosystem resilience during extreme deoxygenation: the Early Jurassic oceanic anoxic event. Oecologia 183, 275–290.

Caswell, B.A., Coe, A.L., Cohen, A.S., 2009. New range data for marine invertebrate species across the early Toarcian (Early Jurassic) mass extinction. Journal J. Geol. Soc., London 166, 859–872.

Cecca, F., Macchioni, F., 2004. The two early Toarcian (Early Jurassic) extinction events in ammonoids. Lethaia 37, 35–56.

Damborenea, S.E., 1987. Early Jurassic Bivalvia of Argentina. Part II: Superfamilies Pteriacea, Buchiacea and part of Pectinacea. Palaeontogr. Abt. A. 99, 113–216. Pl. 1–14.

Damborenea, S.E., 1989. El género *Posidonotis* Losacco (Bivalvia, Jurásico inferior): su distribución estratigráfica y paleogeográfica. Actas 4° Congreso Argentino de Paleontología y Bioestratigrafía (Mendoza) 4, 45–51.

Damborenea, S.E., 1998. The bipolar bivalve *Kolymonectes* in South America and the diversity of Propeamussiidae in Mesozoic times. In: Johnston, P., Haggart, J.W. (Eds.), Bivalves: An Eon of Evolution - Paleobiological Studies Honoring Norman D. Newell. University of Calgary Press, Calgary, pp. 143‑155.

Damborenea, S.E., Manceñido, M.O., 1979. On the palaeogeographical distribution of the pectinid genus *Weyla* (Bivalvia, Lower Jurassic). Palaeogeogr. Palaeoclimatol. Palaeoecol. 27, 85–102.

Damborenea, S.E., Echevarría, J., Ros-Franch, S., 2013. Southern Hemisphere Palaeobiogeography of Triassic-Jurassic Marine Bivalves. Springer Briefs in Earth System Sciences, Springer, Dordrecht. 141 p.

Danise, S., Twitchett, R.J., Little, C.T.S., Clémence, M.E., 2013. The impact of global warming and anoxia on marine benthic community dynamics: an example from the Toarcian (Early Jurassic). PLoS ONE 8, e56255. doi: 10.1371/journal.pone.0056255.

Danise, S., Clémence, M.E., Price, G.D., Murphy, D.P., Gómez, J.J., Twitchett, R.J., 2019. Stratigraphic and environmental control on marine benthic community change through the earlyToarcian extinction event (Iberian Range, Spain). Palaeogeogr. Palaeoclimatol. Palaeoecol. https://doi.org/10.1016/j.palaeo.2019.03.039

Demaison, G.J., Moore, G.T., 1980. Anoxic environments and oil source bed genesis. AAPG Bulletin 64, 1179–1209.

Dera, G., Donnadieu, Y., 2012. Modelling evidences for global warming, Arctic seawater freshening, and sluggish oceanic circulation during the Early Toarcian anoxic event. Paleoceanography 27, PA2211, 1–15.

Dera, G., Pucéat, E., Pellenard, P., Neige, P., Delsate, D., Joachimski, M.M., Reisberg, L., Martinez, M., 2009. Water mass exchange and variations in seawater temperature in the NW Tethys during the Early Jurassic: Evidence from neodymium and oxygen isotopes of fish teeth and belemnites. Earth Planet. Sci. Lett. 286: 198–207.

Dera, G., Neige, P., Dommergues, J.-L., Fara, E., Laffont, R., Pellenard, P., 2010. High-resolution dynamics of Early Jurassic marine extinctions: the case of Pliensbachian-Toarcian ammonites (Cephalopoda). J. Geol. Soc., London 167, 21–33.

Dunhill, A.M., Foster, W.J., Azaele, S., Sciberras, J., Twitchett, R.J. 2018. Modelling determinants of extinction across two Mesozoic hyperthermal events. Proc. R. Soc, B 285: 20180404. https://doi.org/10.1098/rspb.2018.0404

Fantasia, A., Föllmi, K.B., Adatte, T., Bernárdez, E., Spangenberg, J.E., Mattioli, E., 2018. The Toarcian Oceanic Anoxic Event in southwestern Gondwana: an example from the Andean Basin, northern Chile. J. Geol. Soc., London 175, 883–902.

Fraguas, Á., Young, J.R., 2011. Evolution of the coccolith genus *Lotharingius* during the late Pliensbachian-early Toarcian interval in Asturias (N Spain). Consequences of the early Toarcian environmental perturbations. Geobios 44, 361–375.

Fürsich, F.T., Berndt, R., Scheuer, T., Gahr, M., 2001. Comparative ecological analysis of Toarcian (Lower Jurassic) benthic faunas from southern France and east-central Spain. Lethaia 34, 169–199.

García-Joral, F., Gómez, J.J., Goy, A., 2011. Mass extinction and recovery of the Early Toarcian (Early Jurassic) brachiopods linked to climate change in Northern and Central Spain. Palaeogeogr. Palaeoclimatol. Palaeoecol. 302: 367–380.

García Joral, F., Baeza-Carratalá, J.F., Goy, A., 2018. Changes in brachiopod body size prior to the Early Toarcian (Jurassic) Mass Extinction. Palaeogeogr. Palaeoclimatol. Palaeoecol. 506, 242–249.

Gómez, J.J., Goy, A., 2011.Warming-driven mass extinction in the Early Toarcian (Early Jurassic) of northern and central Spain. Correlation with other time-equivalent European sections. Palaeogeogr. Palaeoclimatol. Palaeoecol. 306, 176–195.

Gómez, J.J., Goy, A., Canales, M.L., 2008. Seawater temperature and carbon isotope variations in belemnites linked to mass extinction during the Toarcian (Early Jurassic) in Central and Northern Spain. Comparison with other European sections. Palaeogeogr. Palaeoclimatol. Palaeoecol. 258, 28–58.

Groeber, P., Stipanicic, P., Mingram, A., 1953. Jurásico. In : Geografía de la República Argentina II (1° parte): Mesozoico, p.143–347. Sociedad Argentina de Estudios Geográficos GAEA, Buenos Aires.

Guex, J., Bartolini, A., Spangenberg, J., Vicente, J.C., Schaltegger, U., 2012. Ammonoid multi-extinction crises during the Late Pliensbachian – Toarcian and carbon cycle instabilities. Solid Earth Discussions 4, 1205–1228.

Gulisano, C., Gutiérrez Pleimling, A.R., 1995. Field Guide. The Jurassic of the Neuquén Basin. a) Neuquén Province. Asociación Geológica Argentina Serie E 2; Secretaría de Minería de la Nación, Publicación 158, 1–111.

Hallam, A., 1975. Evolutionary size increase and longevity in Jurassic bivalves and ammonites. Nature 258, 493–496.

Hallam, A., 1977. Jurassic bivalve biogeography. Paleobiology 3, 58–73.

Hallam, A., 1986. The Pliensbachian and Tithonian extinction events. Nature 319, 765–768.

Hallam, A., 1987. Radiations and extinctions in relation to environmental change in the marine Lower Jurassic of northwest Europe. Paleobiology 13, 152–168.

Hallam, A., Wignall, P.B., 1997. Mass Extinctions and their aftermath. Oxford University Press, Oxford. 328 p.

Hammer, Ø., Harper, D.A.T., 2006. Paleontological Data Analysis. Blackwell Publishing, Malden, USA 351 p.

Hammer, Ø., Harper, D.A.T., Ryan, P.D., 2001. PAST: Paleontological Statistics software package for education and data analysis. Palaeontol. Electron. 4(1), 9 p.

Harries, P.J., Little, C.T.S., 1999. The early Toarcian (Early Jurassic) and the Cenomanian-Turonian (Late Cretaceous) mass extinctions: similarities and contrasts. Palaeogeogr. Palaeoclimatol. Palaeoecol. 154, 39–66.

Harries, P.J., Knorr, P.O., 2009. What does the 'Lilliput effect' mean? Palaeogeogr. Palaeoclimatol. Palaeoecol. 284, 4–10.

Hayami, I., 1988. A tethyan bivalve, *Posidonotis dainellii*, from the lower Jurassic of west Japan. Trans. Proc. Palaeont. Soc. Japan, N.S. 151, 564–569.

Hermoso, M., Le Callonnec, L., Minoletti, F., Renard, M., Hesselbo, S.P., 2009. Expression of the Early Toarcian negative carbon-isotope excursion in separated carbonate microfractions (Jurassic, Paris Basin). Earth Planet. Sci. Lett. 277, 194–203.

Hermoso, M., Minoletti, F., Rickaby, R.E., Hesselbo, S.P., Baudin, F., Jenkyns, H.C., 2012. Dynamics of a stepped carbon-isotope excursion: Ultra high-resolution study of Early Toarcian environmental change. Earth Planet. Sci. Lett. 319, 45–54.

Hesselbo, S.P., Gröcke, D.R., Jenkyns, H.C., Bjerrum, C.J., Farrimond, P., Bell, H.S.M., Green, O.R., 2000. Massive dissociation of gas hydrate during a Jurassic oceanic anoxic event. Nature 406, 392–395.

Hesselbo, S.P., Jenkyns, H.C., Duarte, L.V., Oliveira, L.C.V., 2007. Carbon-isotope record of the Early Jurassic (Toarcian) Oceanic Anoxic Event from fossil wood and marine carbonate (Lusitanian Basin, Portugal). Earth Planet. Sci. Lett. 253, 455–470.

Hesselbo, S.P., Korte, C., Ullmann, C.V., 2014. Early-Middle Jurassic chemostratigraphy, black shale, and sea-level change: evidence for cyclically repeated global change events. Beringeria, Special Issue 8, p. 66.

Hönisch, B., Ridgwell, A., Schmidt, D.N., Thomas, E., Gibbs, S.J., Sluijs, A., Zeebe, R., Kump, L., Martindale, R.C., Greene, S.E., Kiessling, W., Ries, J.,. Zachos, J.C., Royer, D.L., Barker, S., Marchitto, T.M. Jr., Moyer, R., Pelejero, C., Ziveri, P., Foster, G.L., Williams, B., 2012. The geological record of ocean acidification. Science 335, 1058–1063.

Iglesia Llanos, M.P., Riccardi, A.C., 2000. The Neuquén composite section: magnetostratigraphy and biostratigraphy of the marine lower Jurassic from the Neuquén basin (Argentina). Earth Planet. Sci. Lett. 181, 443–457.

Izumi, K., Miyaji, T., Tanabe, K., 2012. Early Toarcian (Early Jurassic) oceanic anoxic event recorded in the shelf deposits in the northwestern Panthalassa: Evidence

from the Nishinakayama Formation in the Toyora area, west Japan. Palaeogeogr. Palaeoclimatol. Palaeoecol. 315–316, 100–108.

Jablonski, D., 1996. Body Size and Macroevolution. In: Jablonski, D., Erwin, D.H., Lipps, J.H. (Eds.), Evolutionary Paleobiology. The University Chicago Press. 10, 256–289.

Jenkyns, H.C., 1985. The Early Toarcian and Cenomanian‐Turonian anoxic events in Europe: Comparisons and contrasts. Geol. Rundsch. 74, 505–518.

Jenkyns, H.C., 1988. The Early Toarcian (Jurassic) anoxic event: stratigraphic, sedimentary, and geochemical evidence. Am. J. Sci. 288, 101–151.

Jenkyns, H.C., 2003. Evidence for rapid climate change in the Mesozoic–Palaeogene greenhouse world. Phil. Trans Roy. Soc. London, Series A 361, 1885–1916.

Jenkyns, H.C., 2010. Geochemistry of oceanic anoxic events. Geochem. Geophys. Geosyst. 11, Q03004, 1–30, doi:10.1029/2009GC002788.

Jenkyns, H.C., Clayton, C.J., 1986. Black shales and carbon isotopes in pelagic sediments from the Tethyan Lower Jurassic. Sedimentology 33, 87–106.

Jenkyns, H.C., Clayton, C.J., 1997. Lower Jurassic epicontinental carbonates and mudstones from England and Wales: chemostratigraphic signals and the early Toarcian anoxic event. Sedimentology 44, 687–706.

Kauffman, E.G., Erwin, D.H., 1995. Surviving mass extinctions. Geotimes 14, 14–17.

Kauffman, E.G., Harries, P.J., 1996. The importance of crisis progenitors in recovery from mass extinction. In: Hart, M.B. (Ed.), Biotic Recovery from Mass Extinction Events. Geological Society, London, Spec. Publ. 102, 15–39.

Krencker, F.N., Bodin, S., Suan, G., Heimhofer, U., Kabiri, L., Immenhauser, A., 2015. Toarcian extreme warmth led to tropical cyclone intensification. Earth Planet. Sci. Lett. 425, 120–130.

Leanza, A.F., 1943. *Pectinula*, un nuevo género de pelecípodos en el Lias de Neuquén. Notas Mus. La Plata, Paleont. 8(53), 241–249.

Legarreta, L., Uliana, M.A., 1996. The Jurassic succession in west-central Argentina: stratal patterns, sequences and paleogeographic evolution. Palaeogeogr. Palaeoclimatol. Palaeoecol. 120, 303–330.

Levin, L.A., 2003. Oxygen minimum zone benthos: adaptation and community response to hypoxia. Oceanogr. Mar. Biol. 41, 1–45.

Levinton, J.S., 1970. The paleoecological significance of opportunistic species. Lethaia 3, 69–78.

Levinton, J.S., Bambach, R.K., 1970. Some ecological aspects of bivalve mortality patterns. Am. J. Sci. 268, 97–112.

Little, C.T.S., Benton, M.J., 1995. Early Jurassic mass extinction: a global long-term event. Geology 23, 495–498.

Littler, K., Hesselbo, S.P., Jenkyns, H.C., 2010. A carbon-isotope perturbation at the Pliensbachian–Toarcian boundary: Evidence from the Lias Group, NE England. Geol. Mag. 147, 181–192.

Losacco, U., 1942. Un nuovo genere aaleniano di Aviculidaedella Sabina. Riv. Ital. Paleontol. Stratigr. 48, 9–16.

Macchioni, F., Cecca, F., 2002. Biodiversity and biogeography of middle-late Liassic ammonoids: implications for the early Toarcian mass extinction. Geobios 35 (Mém. Spéc. 24), 165–175.

Manceñido, M.O., Damborenea, S.E., Riccardi, A.C., 2007. The Early Toarcian Oceanic Anoxic Event in the Argentinian Andes. Ameghiniana 44(4), Suplemento Resúmenes, 59R–60R.

Martindale, R.C., Aberhan, M., 2017. Response of macrobenthic communities to the Toarcian Oceanic Anoxic Event in northeastern Panthalassa (Ya Ha Tinda, Alberta, Canada). Palaeogeogr. Palaeoclimatol. Palaeoecol. 478, 103–120.

Maxwell, E.E., Vincent, P., 2015. Effects of the early Toarcian Anoxic Event on ichthyosaur body size and faunal composition in the Southwest German Basin. Paleobiology 42, 117–126.

McElwain, J.C., Wade-Murphy, J., Hesselbo, S.P., 2005. Changes in carbon dioxide during an oceanic anoxic event linked to intrusion into Gondwana coals. Nature 435, 479–482.

McKinney, M.L., 1990. Trends in body-size evolution. In: McNamara, K.J. (Ed.), Evolutionary Trends. University of Arizona Press, Tucson. 75–118.

McKinney, M.L., 1997. Extinction vulnerability and selectivity: combining ecological and paleontological views. Annu. Rev. Ecol. Syst. 28, 495–516.

Monari, S., 1994. I bivalvi giurassici dell´Appennino umbro-marchigiano. In: Biostratigrafía dell´Italia centrale. Universita degli Studi di Camerino, Dipartimento di Scienze della Terra, Camerino, Italy. Stud. Geol. Camerti, Vol. Spec. 157–187.

Morten, S.D., Twitchett, R.J., 2009. Fluctuations in the body size of marine invertebrates through the Pliensbachian-Toarcian extinction event. Palaeogeogr. Palaeoclimatol. Palaeoecol. 284, 29–38.

Oschmann, W., 1993. Environmental oxygen fluctuations and the adaptive response of marine benthic organisms. J. Geol. Soc., London 150, 187–191.

Payne, J.L., 2005. Evolutionary dynamics of gastropod size across the end-Permian extinction and through the Triassic recovery interval. Paleobiology 31, 269–290.

Pedersen, T.F., Calvert, S.E., 1990. Anoxia vs. productivity: what controls the formation of organic-carbon-rich sediments and sedimentary rocks? AAPG Bulletin 74, 454–466.

Percival, L.M.E., Witt, M.L.I., Mather, T.A., Hermoso, M., Jenkyns, H.C., Hesselbo, S.P., Al-Suwaidi, A.H., Storm, M.S., Xu, W., Ruhl, M., 2015. Globally enhanced mercury deposition during the end-Pliensbachian extinction and Toarcian OAE: A link to the Karoo–Ferrar Large Igneous Province. Earth Planet. Sci. Lett. 428, 267–280.

Percival, L.M., Cohen, A.S., Davies, M.K., Dickson, A.J., Hesselbo, S.P., Jenkyns, H.C., Leng, M.J., Mather, T.A., Storm, M.S., Xu, W., 2016. Osmium isotope evidence for two pulses of increased continental weathering linked to Early Jurassic volcanism and climate change. Geology 44, 759–762.

Piazza, V., Duarte, L.V., Renaudie, J., Aberhan, M., 2019. Reductions in body size of benthic macroinvertebrates as a precursor of the early Toarcian (Early Jurassic) extinction event in the Lusitanian Basin, Portugal. Paleobiology, p. 1–21. https://doi.org/10.1017/pab.2019.11

Raup, D.M., Sepkoski, J.J.Jr., 1984. Periodicity of extinctions in the geologic past. PNAS 81, 801–805.

Riccardi, A.C., 2005. First teuthid cephalopod from the Lower Jurassic of South America (Neuquén Basin, Argentina). Geol. Acta 3, 179–184.

Riccardi, A.C., 2008a. The marine Jurassic of Argentina: a biostratigraphic framework. Episodes 31, 326–335.

Riccardi, A.C., 2008b. El Jurásico de Argentina y sus amonites. Rev. Asoc. Geol. Argent. 63, 625–643.

Riccardi, A.C., Damborenea, S.E. (Eds.),1993. Léxico Estratigráfico Argentino. Volumen IX. Jurásico. Asociación Geológica Argentina, Serie B (Didáctica y Complementaria) 21, 1–477.

Röhl, H.J., Schmid-Röhl, A., Oschmann, W., Frimmel, A., Schwark, L., 2001. The Posidonia Shale (Lower Toarcian) of SW Germany: an oxygen-depleted ecosystem controlled by sea level and palaeoclimate. Palaeogeogr. Palaeoclimatol. Palaeoecol. 165, 27–52.

Ros-Franch, S., Damborenea, S.E., Al-Suwaidi, A., Hesselbo, S.P., Jenkyns, H.C., Manceñido, M.O., Riccardi, A.C., 2014. Relationship between anoxic conditions and size in *Posidonotis* (Bivalvia) from the Lower Jurassic of the Neuquén Basin, Argentina. Fourth International Palaeontological Congress, Abstract Volume, 800.

Schmid-Röhl, A., Röhl, H.-J., Oschmann, W., Frimmel, A., Schwark, L., 2002. Palaeoenvironmental reconstruction of Lower Toarcian epicontinental black shales (Posidonia Shale, SW Germany): global versus regional control. Geobios 35, 13–20.

Sepkoski, J.J.Jr, Raup, D.M., 1986. Periodicty of marine extinction events. In: Elliott, D.K. (Ed.), Dynamics of extinction. Wiley, New York, 3–36.

Tanabe, K., 1991. Early Jurassic Macrofauna of the Oxygen-Depleted Epicontinental Marine Basin in the Toyora Area, West Japan. Saito Ho-On Kai, Spec. Publ. 3 (Proceedings of Shallow Tethys 3, Sendai, 1990), 147–161.

Trecalli, A., Spangenberg, J., Adatte, T., Föllmi, K.B., Parente, M., 2012. Carbonate platform evidence of ocean acidification at the onset of the early Toarcian oceanic anoxic event. Earth Planet. Sci. Lett. 357, 214–225.

Twitchett, R.J., 2007. The Lilliput effect in the aftermath of the end-Permian extinction event. Palaeogeogr. Palaeoclimatol. Palaeoecol. 252, 132–144.

Uliana, M.A., Biddle, K.T., 1988. Mesozoic-Cenozoic paleogeographical and geodynamic evolution of southern South America. Rev. Bras. Geociênc. 18, 172–190.

Ullmann, C.V., Thibault, N., Ruhl, M., Hesselbo, S.P., Korte, C., 2014. Effect of a Jurassic oceanic anoxic event on belemnite ecology and evolution. PNAS 111, 10073–10076.

Vergani, G.D., Tankard, A.J., Belotti, H.J., Welsink, H.J., 1995. Tectonic evolution and paleogeography of theNeuquen Basin, Argentina. In: Tankard, A.J., Suarez Soruco, R., Welsink, H.J. (Eds.), Petroleum Basins of South America. Am. Assoc. Pet. Geol. Mem. 62, 383–402.

Volkheimer, W., 1973. Palinología estratigráfica del Jurásico de la Sierra de Chacai Coy adyacencias (Cuenca Neuquina, República Argentina). I. Estratigrafía de las Formaciones Sierra Chacai Co (Pliensbachiano), Los Molles (Toarciano, Aaleniano), Cura Niyeu (Bayociano) y Lajas (Caloviano Inferior). Ameghiniana 10, 85–131.

Weaver, C., 1931. Paleontology of the Jurassic and Cretaceous of West Central Argentina. Memoir of the University of Washington 1, 496 p.

Wignall, P.B., Newton, R.J., Little, C.T.S., 2005. The timing of paleoenvironmental change and cause-and-effect relationships during the Early Jurassic mass extinction in Europe. Am. J. Sci. 305, 1014–1032.

Xu, W., Ruhl, M., Jenkyns, H.C., Leng, M.J., Huggett, J.M., Minisini, D., Ullmann, C.V., Riding, J.B., Weijers, J.W., Storm, M.S., Percival, L.M., 2018. Evolution of the Toarcian (Early Jurassic) carbon-cycle and global climatic controls on

local sedimentary processes (Cardigan Bay Basin, UK). Earth Planet. Sci. Lett. 484, 396–411.

Figure captions:

Figure 1.A- Latest Pliensbachian-earliest Toarcian global palaeogeography (modified after Cao et al., 2017); B-Location of Arroyo Lapa section in Neuquén Basin, Argentina (local palaeogeogaphy modified after Legarreta and Uliana, 1996). Both with location of *Posidonotis* occurrences (stars).

Figure 2. **A**. Location of the Arroyo Lapa South logged section (line) (satellite image courtesy of Google Earth). **B**. General view of the studied succession at Arroyo Lapa South section (persons for scale). **C**. Detail of beds with *Posidonotis cancellata* (Leanza), coin diameter 18.2 mm.

Figure 3: Measurements of *Posidonotis cancellata* (Leanza), MLP 35885. Abbreviations: L, length; H, height. Dashed line shows outline of measured shell-surface.

Figure 4: General aspect of slabs with different densities of specimens of *Posidonotis cancellata* (Leanza), all to the same scale. **A**, sparse, specimens separated by a distance larger than their size, MLP 35888; **B**, low density, specimens separated by distances shorter than their size, MLP 35888; **C**, high density, specimens in contact, covering almost all surface, MLP 35900; **D**, highest density overlapping valves covering entire surface, MLP 35885.

Figure 5: Logged section at Arroyo Lapa (Neuquén Basin, Argentina), showing beds with *Posidonotis cancellata*, $d^{13}C$ values from bulk sediment, %TOC profile, median and maximum length values, and abundance data for samples of *P. cancellata* with 5 or

more shells. General section (left, logged by Damborenea and Manceñido), and detailed section of the Pliensbachian–Toarcian boundary beds (right, logged by Al-Suwaidi et al., 2010). Local ammonite biostratigraphy by A.C. Riccardi. Solid lines in geochemical curves correspond to data used in this analysis, published by Al-Suwaidi et al. (2010); broken lines are additional data for the upper part of the section published by Al-Suwaidi et al. (2016). Grey background indicates T-OAE (*sensu* Al-Suwaidi et al., 2010, 2016).

Figure 6: Histograms showing the size (in millimetres) frequencies distribution for samples lumped under increasing and decreasing %TOC (top) and $\delta^{13}C$ (bottom) conditions.

Table 1: Main data for *Posidonotis cancellata* and geochemical variables considered for the analyses. Bold values in the first column indicates the coincidence between *P. cancellata* and geochemical samples. *dif. %TOC*= first %TOC value after the *Posidonotis* sample minus immediate previous value; *dif.* $\delta^{13}C_{org}$=first $\delta^{13}C_{org}$ value after the *Posidonotis* sample minus immediate previous value (see text).

Table 2: Results of the Spearman rank-order correlation analyses.
r_s: Spearman's coefficient; *p*: probability of non-correlation; *****: significant values.
dif. %TOC= first %TOC value after the *Posidonotis* sample minus immediate previous value; *dif.* $\delta^{13}C_{org}$=first $\delta^{13}C_{org}$ value after the *Posidonotis* sample minus immediate previous value (see text).

					length (mm)									geochemical proxies			
collection number	dist. from base (m)	N	Abundance (ind/dm²)	Abundance (surf/surf)	5 maximum lengths					Median	Variance	Skewness	Kurtosis	$\delta^{13}C$	dif. $\delta^{13}C$	%TOC	dif. %TOC
MLP35870	**24.55**	11	7.2	0.14	17.5	17.1	16.8	16.6	16.6	12.0	26.1	-0.30	-1.82	-27.45	-0.64	0.34	-1.71
MLP35871	33.1	14	12.4	0.24	20.8	18.9	17.5	17.5	16.6	14.9	9.8	0.23	-0.88	-24.73	-0.59	2.28	1.67
MLP35873	**36.05**	5	7.9	0.20	17.5	13.6	13.0	12.4	10.1	13.0	7.1	0.81	1.94	-26.24	0.55	3.66	2.84
MLP35874-MLP35876	36.35	60	29.2	0.40	24.6	23.0	22.8	20.6	19.7	11.7	22.1	0.48	-0.44	-26.63	-0.39	4.07	0.40
MLP35878	**39.05**	21	18.3	0.34	17.8	16.8	16.0	15.1	14.7	12.5	9.4	-0.03	-1.13	-26.91	-1.04	3.20	-0.09
MLP35879	42.45	25	40.2	0.44	20.3	19.2	18.7	15.3	13.4	9.6	19.9	0.84	0.12	-26.65	-2.43	4.25	2.02
MLP35881	42.85	6	24.5	0.52	10.9	10.9	10.7	8.7	7.3	9.7	3.5	-0.36	-2.49	-25.53	1.12	3.62	-0.63
MLP35882	**43.05**	8	26.0	0.28	14.8	13.7	10.9	10.2	9.7	10.0	10.1	0.17	-0.55	-25.53	1.12	3.62	-0.63
MLP35883-MLP34884	**46.05**	27	11.0	0.16	16.7	16.6	14.4	13.7	13.4	10.2	11.1	0.04	-0.41	-24.30	0.29	3.05	-0.84
MLP35885	**54.55**	168	51.4	0.62	24.3	21.0	20.9	19.8	19.1	13.3	13.1	0.08	-0.42	-26.78	-4.89	2.63	0.55
MLP35887-MLP35888	54.65	84	63.4	0.68	20.7	20.7	19.3	19.3	17.9	12.0	12.3	0.30	0.18	-26.78	0.47	2.63	1.68
MLP35886	**55.55**	7	64.3	0.71	17.1	16.5	13.9	13.5	13.3	13.5	5.6	0.05	-0.38	-26.81	-0.50	4.88	0.57
MLP35890	55.85	15	56.6	0.52	18.2	14.1	13.1	12.2	11.1	10.6	9.1	1.09	1.69	-25.43	1.38	4.06	-0.82
MLP35892	56.65	7	22.0	0.36	15.6	15.5	14.5	13.5	12.1	13.5	9.7	-1.45	2.34	-25.87	0.43	2.73	-0.98

MLP35893	57.3	12	34.7	0.88	15.1	14.0	13.3	13.1	12.3	11.6	4.6	-0.46	0.42	-25.44	-0.46	1.75	0.31
MLP35894	57.65	5	23.2	0.24	12.4	9.6	8.7	8.3	5.3	8.7	6.5	0.00	1.37	-25.90	-0.61	2.06	2.35
MLP35895	**61.05**	22	27.8	0.39	17.6	15.5	12.2	12.0	12.0	10.0	7.8	1.20	1.64	-27.88	-1.00	4.36	-1.97
MLP35896	**61.55**	8	25.9	0.29	18.8	15.5	15.0	13.3	12.5	12.9	12.9	-0.22	0.88	-27.91	-0.03	5.67	1.31
MLP35897	61.85	7	6.2	0.14	20.7	20.6	16.9	15.8	14.1	15.8	23.1	-0.32	-1.11	-28.48	-0.57	0.62	-5.05

Table 1 - Main data for *Posidonotis cancellata* and geochemical variables considered for the analyses. Bold values in the second column indicates the coincidence between *P. cancellata* and geochemical samples. ***dif. %TOC***= first %TOC value after the Posidonotis sample minus immediate previous value; ***dif.*** $\boldsymbol{\delta^{13}C}$=first δ^{13}C value after the Posidonotis sample minus immediate previous value (see text).

		$\delta^{13}C$	dif. $\delta^{13}C$	%TOC	dif. %TOC
max. length	r_s	-0.36	-0.36	0.06	0.14
	p	0.13	0.13	0.79	0.56
5 max. length	r_s	-0.28	-0.36	-0.12	0.06
	p	***0.01	***0.00	0.25	0.57
median	r_s	-0.28	-0.08	-0.21	-0.06
	p	0.25	0.73	0.39	0.80
variance	r_s	-0.40	-0.30	-0.17	-0.16
	p	0.09	0.22	0.49	0.50
skewness	r_s	0.04	-0.02	0.50	0.31
	p	0.86	0.92	***0.03**	0.20
kurtosis	r_s	0.12	0.23	0.31	0.24
	p	0.63	0.34	0.19	0.31
Abundance (ind/dm²)	r_s	0.03	0.05	0.45	0.29
	p	0.90	0.84	0.06	0.23
Abundance (surf/surf)	r_s	0.09	0.06	0.31	0.22
	p	0.71	0.82	0.20	0.37

Table 2 - Results of the Spearman rank-order correlation analyses.
r_S: Spearman's coefficient; *p*: probability of non-correlation; ***:** significant values.
dif. %TOC= first %TOC value after the Posidonotis sample minus immediate previous value; ***dif. $\delta^{13}C$***=first $\delta^{13}C$ value after the Posidonotis sample minus immediate previous value (see text).

HIGHLIGHTS

- *P. cancellata* size and abundance data from Toarcian relate to OAE geochemical proxies
- Shell size correlates positively with %TOC, probably linked to primary productivity
- Maximum abundance at the onset of the T-OAE, and then decreasing until its extinction
- *P. cancellata* shows opportunistic species features, but with a low juvenile mortality

P. cancellata anatomical features suggest adaptation to dysaerobic environments.

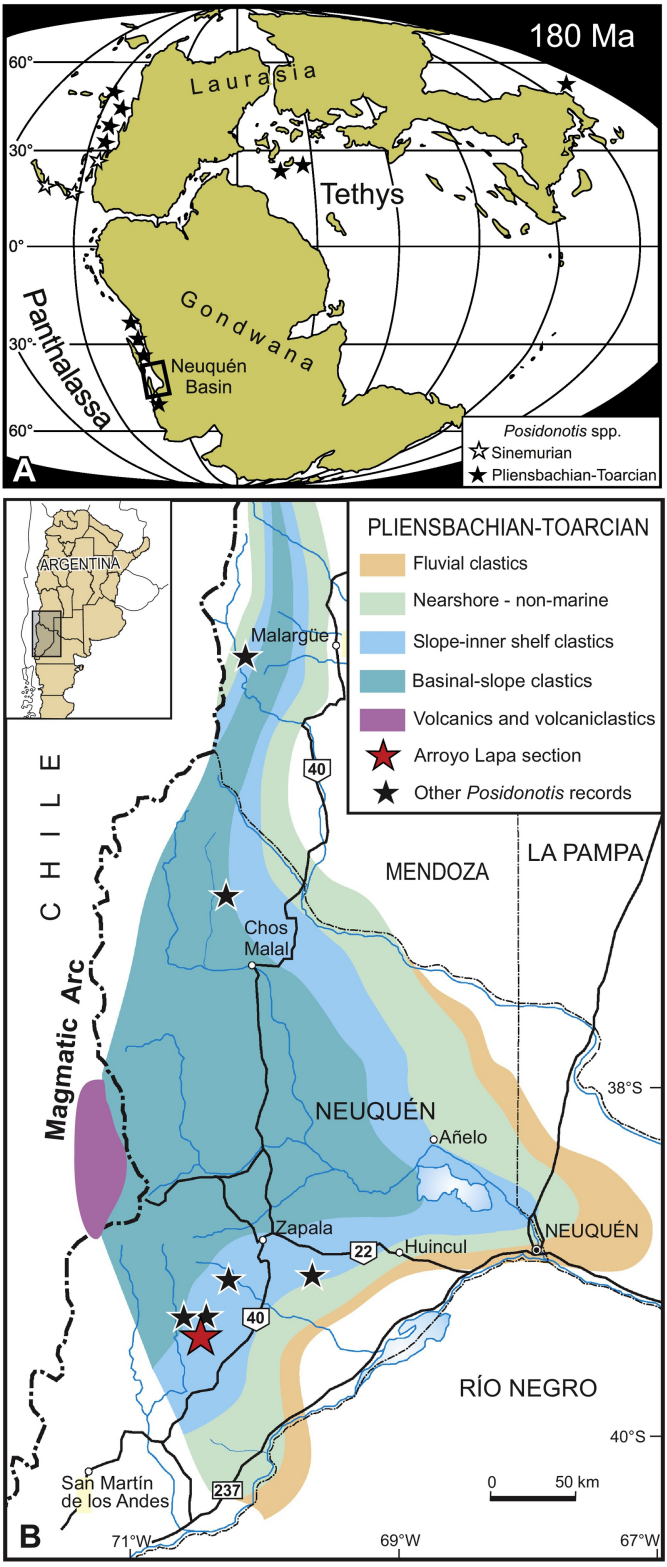
180 Ma
Laurasia
Tethys
Gondwana
Panthalassa
Neuquén Basin
60°
30°
0°
30°
60°
Posidonotis spp.
Sinemurian
Pliensbachian-Toarcian
A
ARGENTINA
PLIENSBACHIAN-TOARCIAN
Fluvial clastics
Nearshore - non-marine
Slope-inner shelf clastics
Basinal-slope clastics
Volcanics and volcaniclastics
Arroyo Lapa section
Other Posidonotis records
Malargüe
CHILE
Magmatic Arc
40
MENDOZA
LA PAMPA
Chos Malal
NEUQUÉN
38°S
Añelo
Zapala
22
Huincul
NEUQUÉN
40
RÍO NEGRO
40°S
San Martín de los Andes
237
0
50 km
B
71°W
69°W
67°W

Figure 1

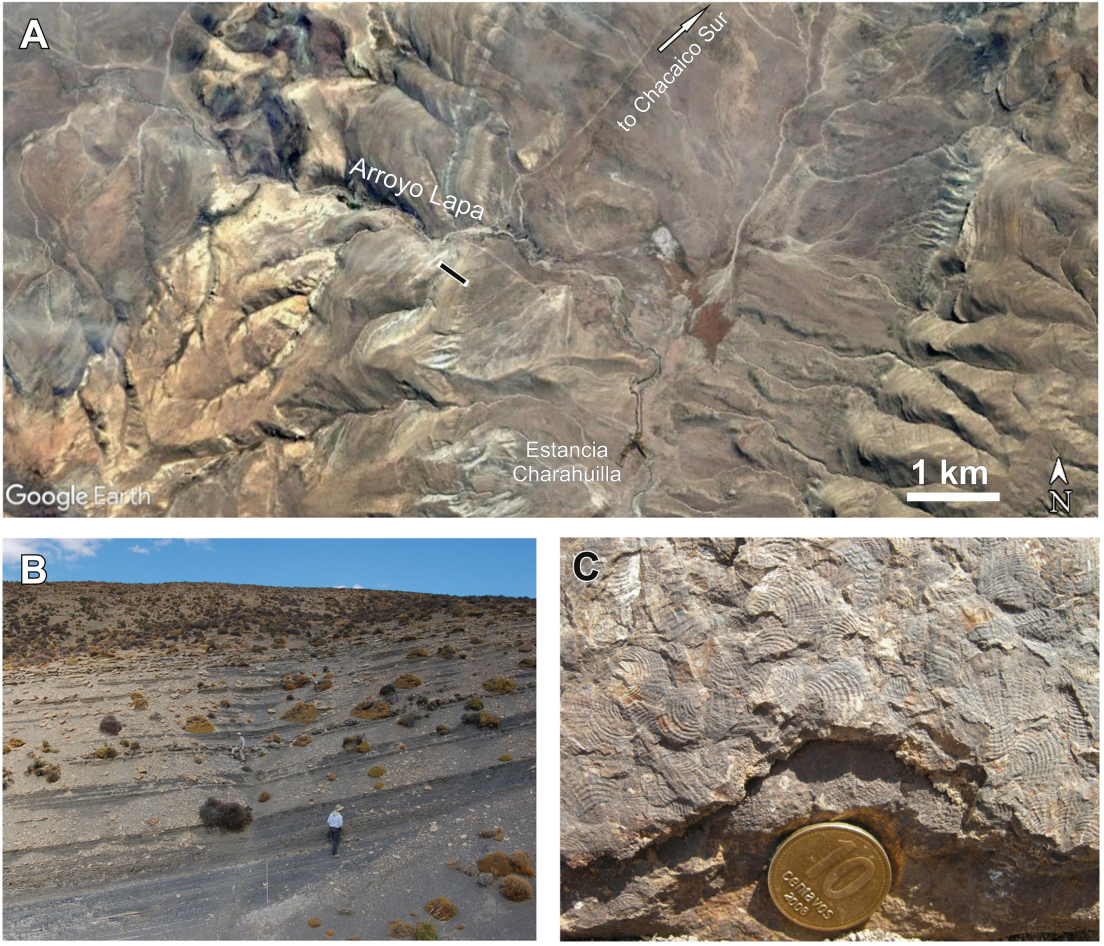
A
to Chacaico Sur
Arroyo Lapa
Estancia
Charahuilla
Google Earth
1 km
N
B
C
10
centavos

Figure 2

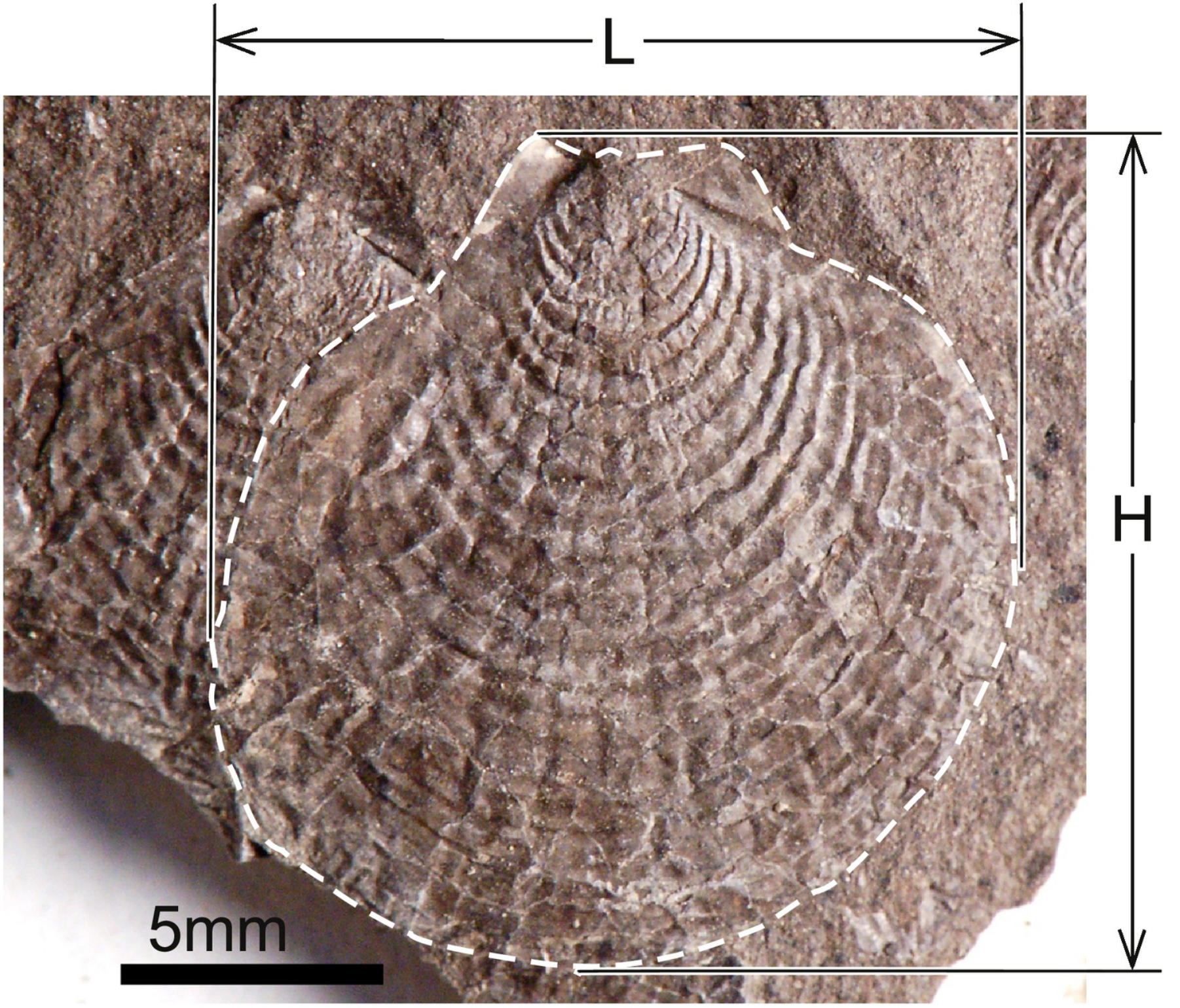

Figure 3

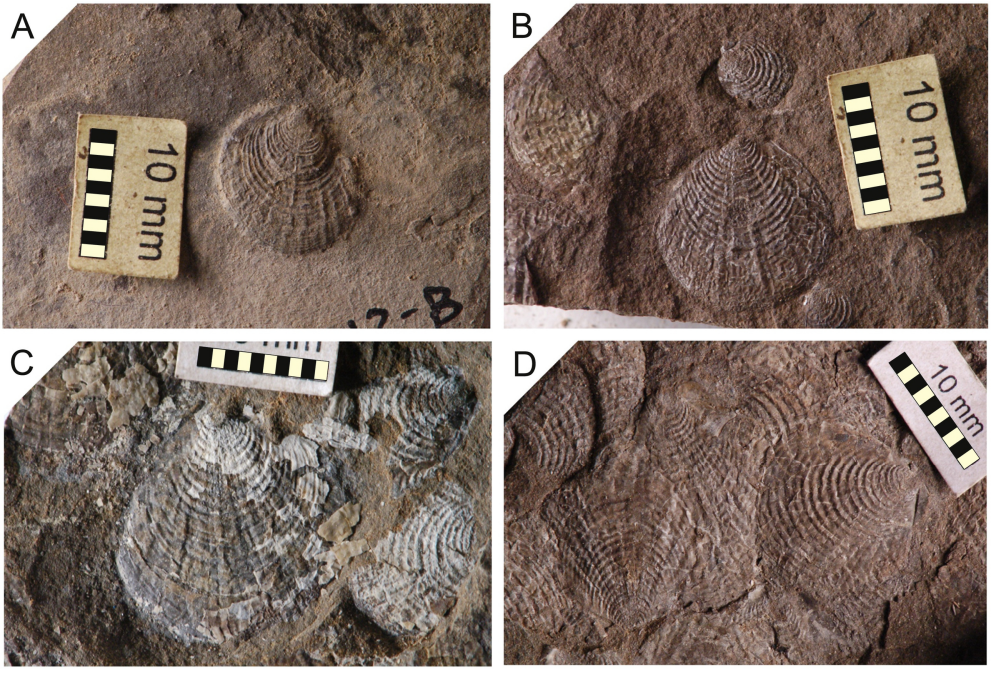

Figure 4

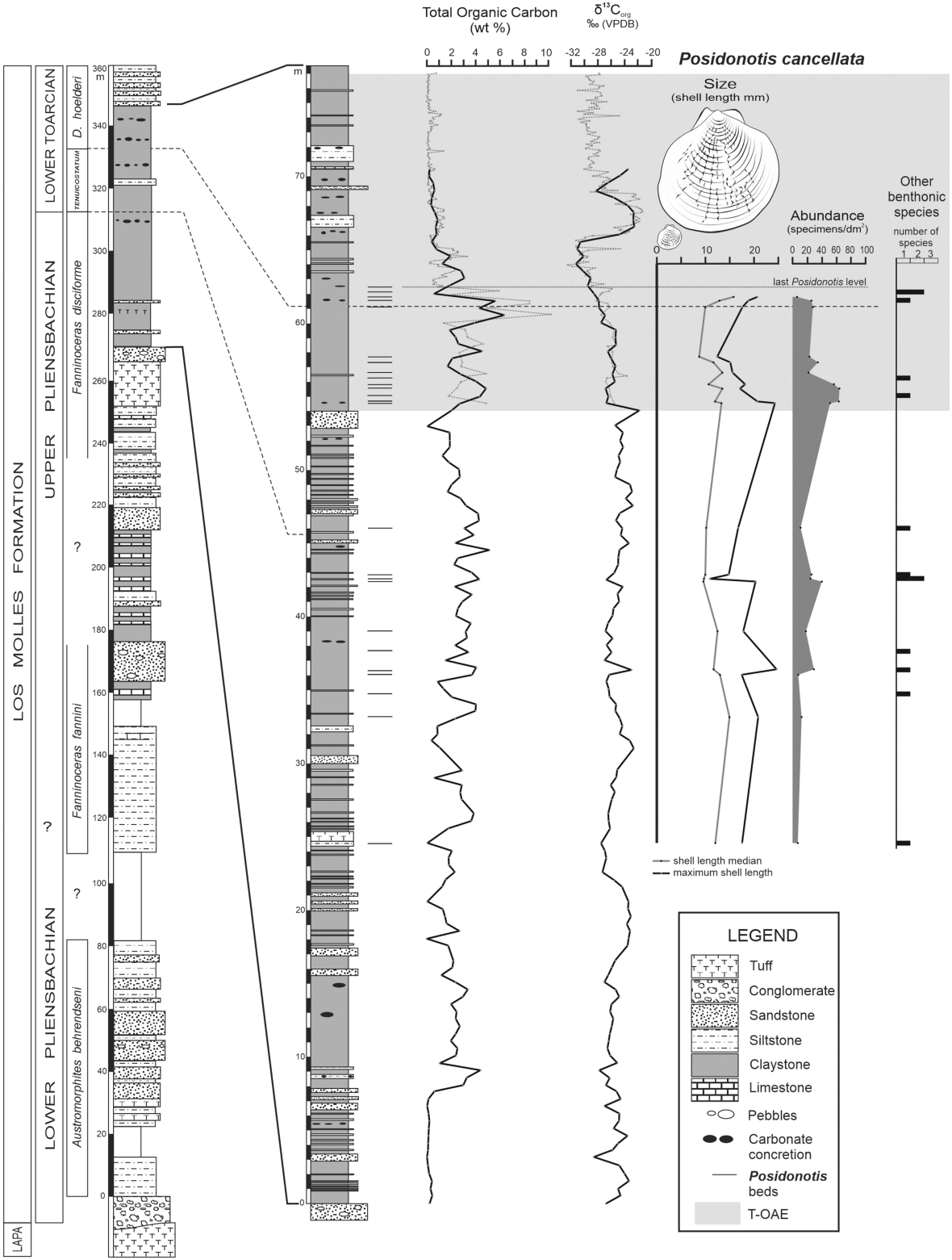
Total Organic Carbon (wt %)
$\delta^{13}C_{org}$ ‰ (VPDB)
Posidonotis cancellata
Size (shell length mm)
Abundance (specimens/dm²)
Other benthonic species
number of species
last Posidonotis level
shell length median
maximum shell length
LOS MOLLES FORMATION
LOWER TOARCIAN
UPPER PLIENSBACHIAN
LOWER PLIENSBACHIAN
LAPA
D. hoelderi
TENUICOSTATUM
Fanninoceras disciforme
Fanninoceras fannini
Austromorphites behrendseni
LEGEND
Tuff
Conglomerate
Sandstone
Siltstone
Claystone
Limestone
Pebbles
Carbonate concretion
Posidonotis beds
T-OAE

Figure 5

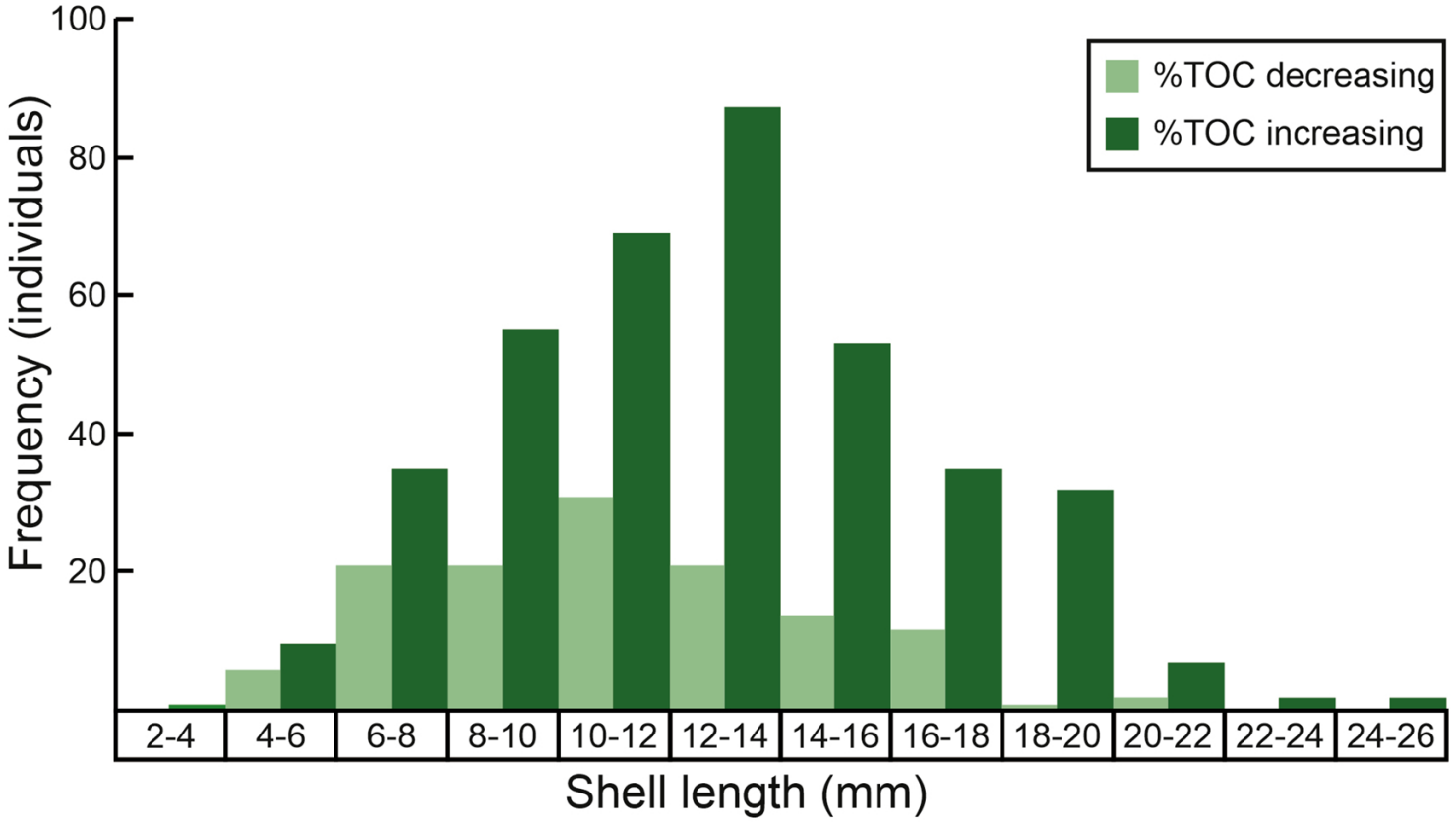
100
80
60
40
20
Frequency (individuals)
%TOC decreasing
%TOC increasing
2-4
4-6
6-8
8-10
10-12
12-14
14-16
16-18
18-20
20-22
22-24
24-26
Shell length (mm)

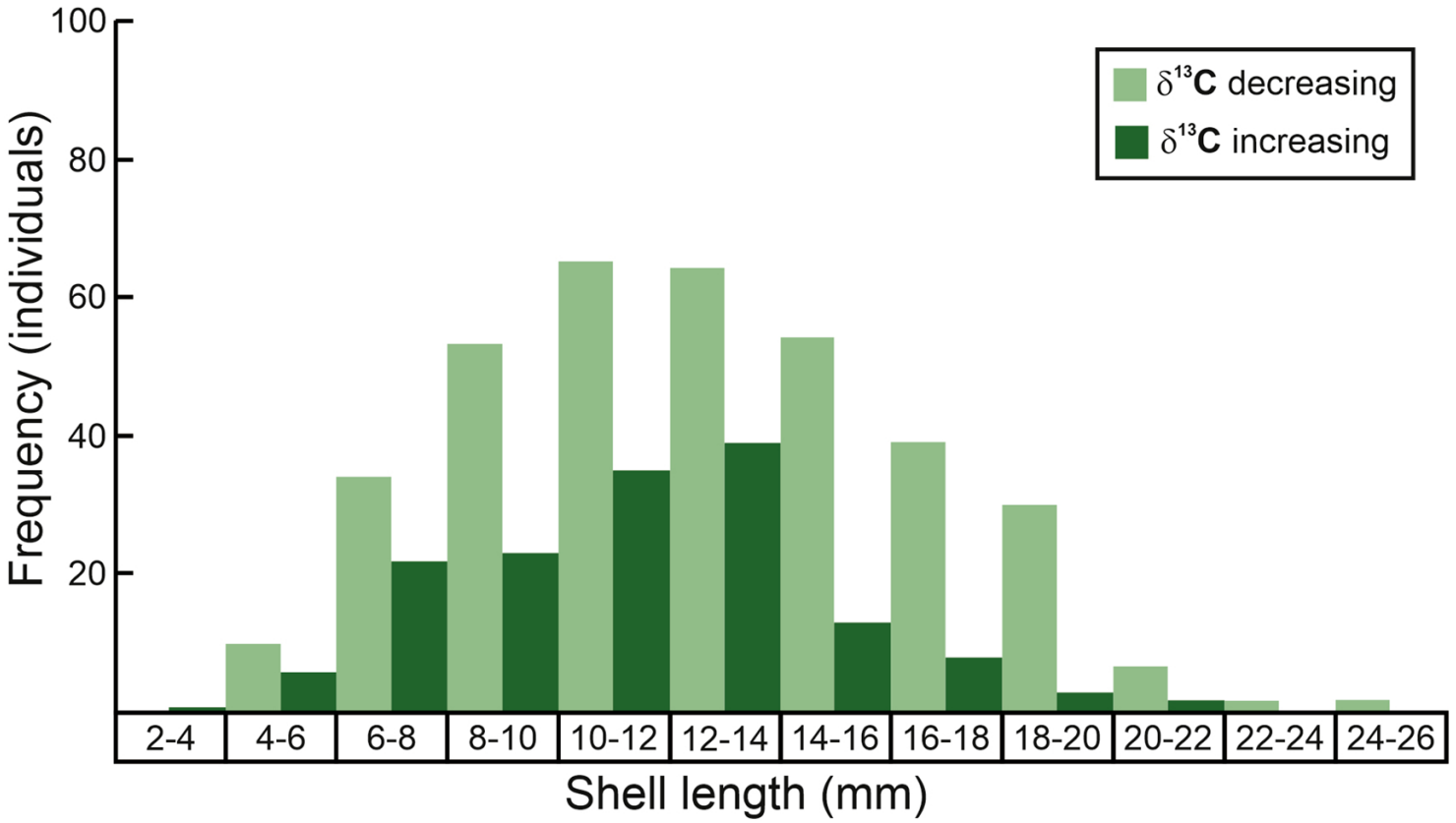
100
80
60
40
20
Frequency (individuals)
δ13C decreasing
δ13C increasing
2-4
4-6
6-8
8-10
10-12
12-14
14-16
16-18
18-20
20-22
22-24
24-26
Shell length (mm)

Figure 6